Numerical Simulation of a two-dimensional internal wave attractor

Nicolas Grisouard†, Chantal Staquet†, Ivane Pairaud†,‡
† Laboratoire des Écoulements Géophysiques et Industriels, Grenoble, France
‡ (present address) LER PAC, Ifremer Toulon, France
contact : +33 (0)476 825 037, nicolas.grisouard@hmg.inpg.fr

Introduction

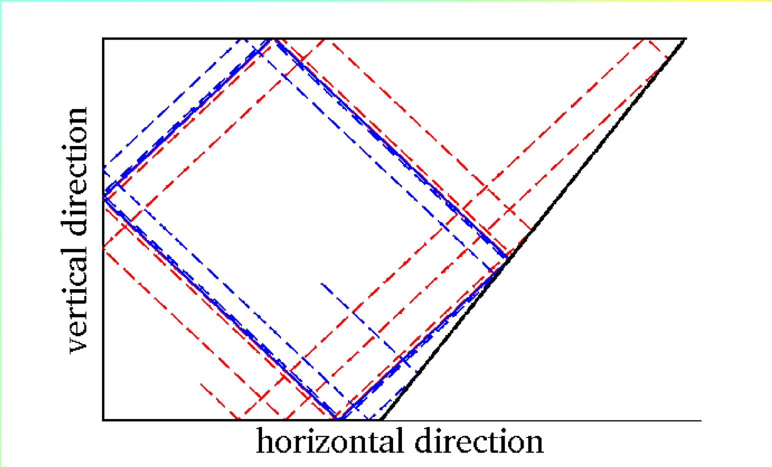

Fig. 1: geometrical focusing of internal gravity wave beams in a closed domain with constant N. Due to the reflection property at the sloping wall, rays (red and blue) are focused and eventually get close to a pattern called wave attractor.

Internal wave attractors may form in **stably stratified fluids** enclosed in containers that have **non-normal or non-parallel boundaries with respect to gravity** (see [3]). Such configurations could be relevant for astrophysical bodies, some closed areas of the deep ocean and lakes. The dispersion relation of the internal waves, namely $\omega = N\cdot\cos\theta$, relates the temporal frequency of the waves ω to the angle of propagation of the energy with respect to the direction of gravity θ in a given medium of Brunt-Väisälä frequency N. This anisotropic relation leads to a peculiar reflexion property which is responsible for the existence of internal wave attractors (see fig. 1). Hazewinkel *et al.* (2008) (HBDM08, [2]) recently performed new laboratory experiments of a wave attractor. Our purpose is to present the result of a 2D direct numerical simulation of one of these experiments using the **MIT general circulation model**.

Numerical Set-Up

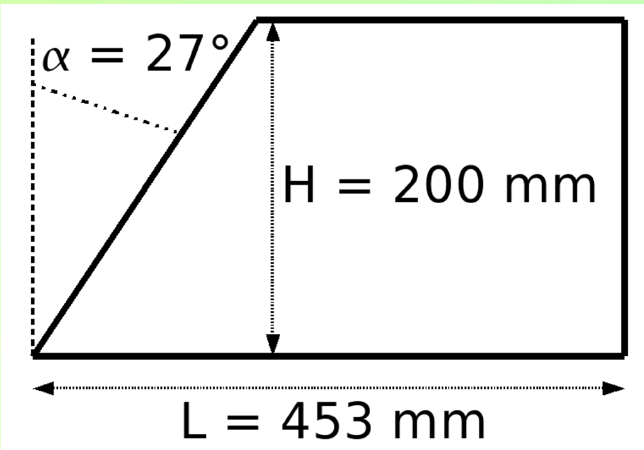

Fig. 2: Physical dimensions of the tank

The MITgcm code is used in a **two-dimensional non-hydrostatic, non-linear DNS configuration.** The spatial scheme is an explicit finite volume method and the temporal scheme is an order 3 Adams-Bashforth method. The Boussinesq approximation is assumed.

Starting from rest, a horizontal oscillating current of frequency ω is applied at the vertical boundary during 61T. The forcing is then relaxed and the field decays.

Grid size	908 x 400 pts²
dx, *dz* (spatial resolution)	0.5 mm
ν (viscosity)	1 mm²/s
κ (diffusivity)	0.01 mm²/s
N (Brunt-Väisälä frequency)	2.76 rad/s
ω (forcing frequency)	1.23 rad/s
T (forcing period)	5.11 s
U (amplitude of forcing)	$7.38 \cdot 10^{-2}$ mm/s
dt (temporal resolution)	0.02044 s, T/250
Boundary conditions	Free slip, free surface

Validation of the simulation : comparison with HBDM08's experiment

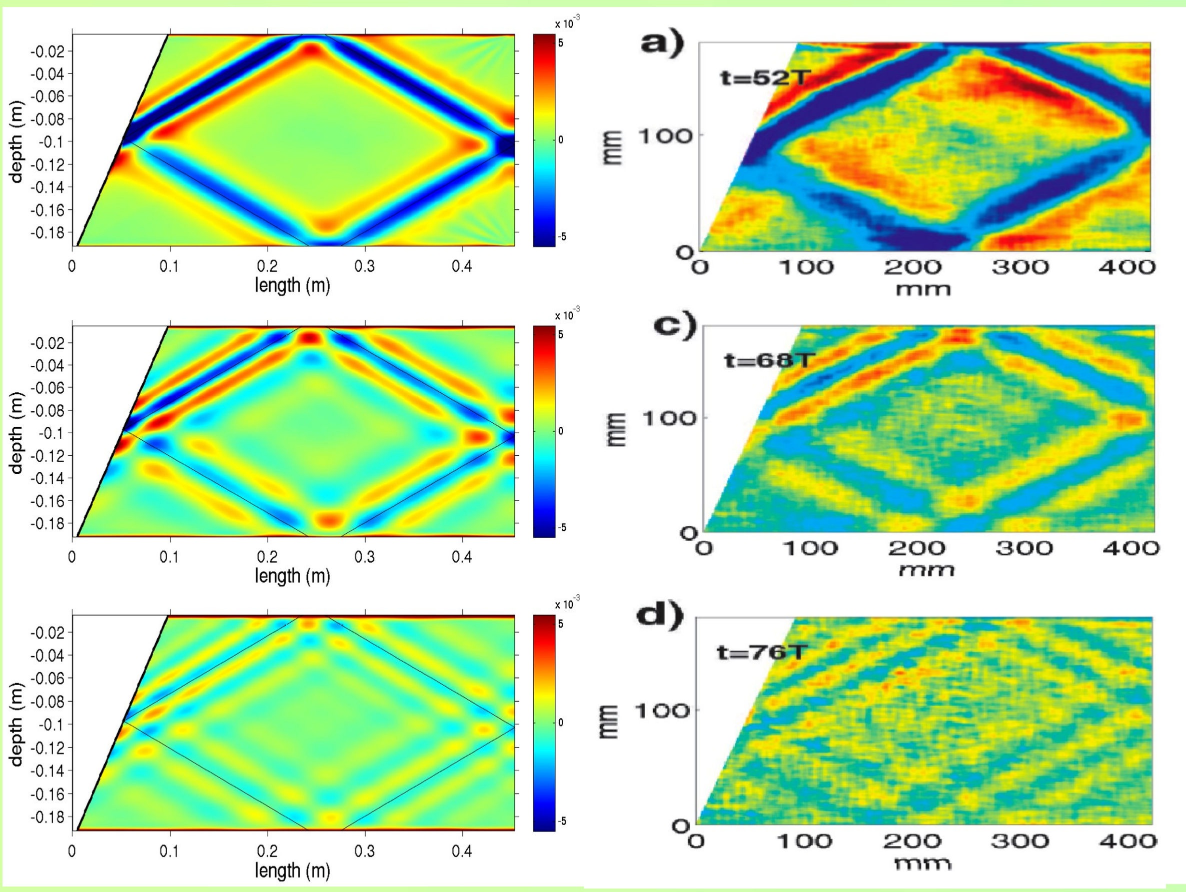

The overall behavior of the fluid motions is **well reproduced** by the model. First, the attractor grows for approximately 30T, followed by a stationary phase and finally a decay stage, with a few snapshots displayed in fig. 3. In the following we focus on the stationary regime.

Fig. 3: Constant contours of $\partial_z b$ (b being the buoyancy) at different times during the decay stage. Left: output of the simulation; right: laboratory experiments of HBDM08. Top: 2T after the forcing has been turned off; middle: 18T ; bottom: 26T.

A refined analysis, from the computation of spatial spectra along four different sections across the attractor (fig. 4), still reveals discrepancies: the **viscous damping** seems to be more efficient in the laboratory. The viscous dissipation at the sidewalls in the laboratory, not taken into account in our 2D configuration, might be a more powerful sink of energy than expected.

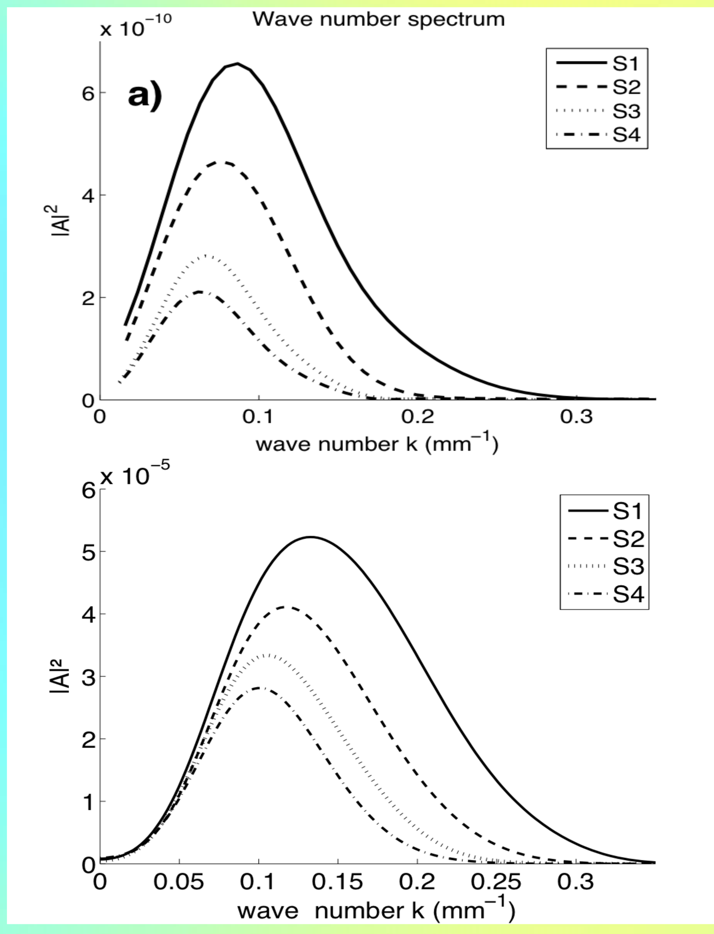

Fig. 4: Spatial spectral analysis of $\partial_z b$ along four different sections across the attractor during the permanent regime. S1 is located in the middle of the first branch, S4 in the middle of the fourth branch. Top: HBDM08 ; bottom : output of our simulation.

Thickness of the attractor

The width of the attractor λ may be assumed to result from a **balance between focusing and viscous broadening** (see [4], [2]). As shown in [1], this leads to the following expression for λ:

$$\lambda \propto \left(\frac{s\nu}{L_a}+\frac{\nu}{\gamma^3-1}\right)^{1/3}$$

s being the along-branches coordinate, L_a the length of the attractor and γ the focusing factor.

If $\gamma \gg 1$, the theoretical prediction by [5] is recovered implying that, in the fluid reference frame, **the attractor can be seen as a beam emitted by the** (now oscillating) **inclined wall.**

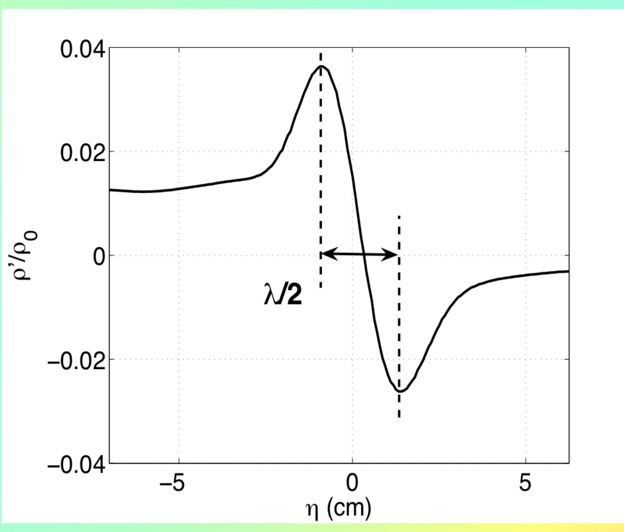

Fig. 5: cross-section of the attractor in the middle of S1.

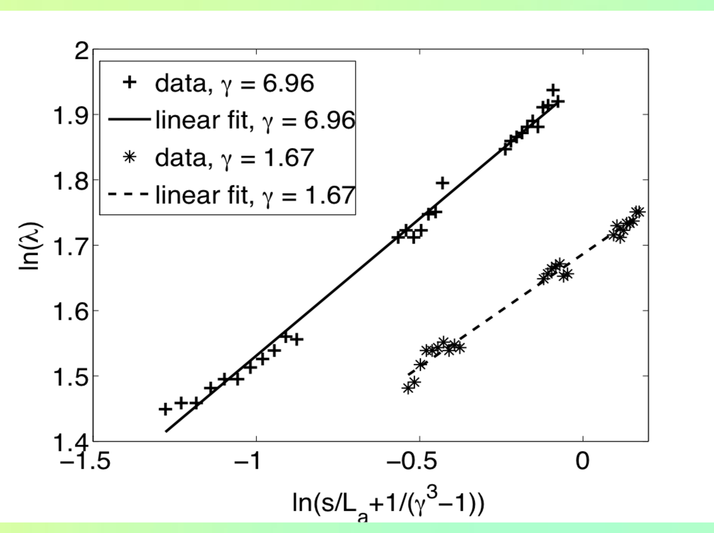

Fig. 6: evolution of λ along the branches of the attractor for two different sets of parameters. Dashed line: the computed exponent is 0.23 (instead of 1/3). Solid line: other set of parameters, the computed exponent is 0.42.

References
[1]Grisouard N., Staquet C., Pairaud I., Numerical simulation of a two-dimensional internal wave attractor, *submitted to J. Fluid Mech.*
[2]Hazewinkel J., van Breevoort P., Dalziel S.B. & Maas L.R.M. 2008, Observations on the wave number spectrum and evolution of an internal wave attractor in a two-dimensional basin, *J. Fluid Mech*, **598**, 373-382
[3]Maas L.R.M & Lam F-P.A. 1995, Geometric focusing of internal waves, *J. Fluid Mech*, **300**, 1-41
[4]Rieutord M., Georgeot B. & Valdettaro L. 2001, Inertial waves in a rotating spherical shell: attractor and asymptotic spectrum, *J. Fluid Mech.*, **435**, 104-144
[5]Thomas N.H. & Stevenson T.N. 1972, a similarity solution for viscous internal waves, *J. Fluid Mech.*, **54**, part 3, 495-506

Acknowledgments: We thank Leo Maas and Jeroen Hazewinkel for proposing us to model numerically the internal wave attractor, for having provided an earlier draft of the experimental paper and for the fruitful discussions. Computations were performed on the French Supercomputer Center IDRIS.

Non-linear effects

If we now multiply U by 10, **non-linearities and harmonics generation** become more visible. By temporally filtering the signal during the permanent regime, it is possible to isolate the signal of every frequency, as can be seen in fig. 7. Beams of frequency 2ω can be seen. On the otherhand, $3\omega > N$ so the second harmonic remains locally confined.

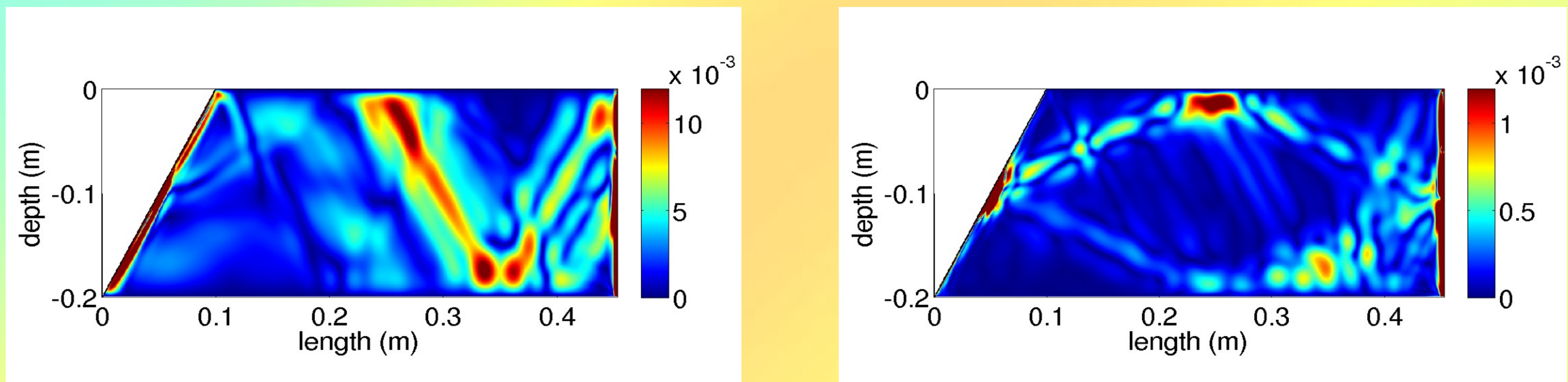

Fig.7: temporal filtering of $\partial_z b$ during the permanent regime. Left: amplitude of the first harmonic (2ω); right : amplitude of the confined second harmonic (3ω).

Conclusion

Summary:
- Successful non-linear, non-hydrostatic numerical reproduction of the laboratory experiment of HBDM08
- Careful comparison of the two sets of data
- Theoretical modeling of the width of the attractor, confirmed by the numerical results
- Evidence of the existence of non-linear effects and harmonics generation

Perspectives:
- To carry on new experiments about non-linearities and mixing
- To address geophysical situations